Practical Field Alignment of Parabolic Trough Solar Concentrators

Richard B. Diver
e-mail: rbdiver@sandia.gov

Timothy A. Moss
e-mail: tamoss@sandia.gov

Sandia National Laboratories,
P.O. Box 5800, MS1127,
Albuquerque, NM 87185

In this paper a new technique for parabolic trough mirror alignment based on the use of an innovative theoretical overlay photographic (TOP) approach is described. The technique is a variation on methods used to align mirrors on parabolic dish systems. It involves overlaying theoretical images of the heat collection element (HCE) in the mirrors onto carefully surveyed photographic images and adjustment of mirror alignment until they match. From basic geometric principles, for any given viewer location the theoretical shape and location of the reflected HCE image in the aligned mirrors can be predicted. The TOP approach promises to be practical and straightforward, and inherently aligns the mirrors to the HCE. Alignment of an LS-2 mirror module on the rotating platform at the National Solar Thermal Test Facility (NSTTF) with the TOP technique along with how it might be implemented in a large solar field is described. Comparison of the TOP alignment to the distant observer approach on the NSTTF LS-2 is presented and the governing equations used to draw the theoretical overlays are developed. Alignment uncertainty associated with this technique is predicted to be less than the mirror slope error. [DOI: 10.1115/1.2710496]

Keywords: parabolic trough, solar concentrator, alignment, photographic, overlay, reflection

Introduction

Parabolic trough solar concentrators have been developed, fielded, and are currently producing clean solar-generated electricity in southern California [1,2]. Additional trough projects are currently at various stages of development in Nevada and Spain [3,4]. Most trough concentrators use multiple mirror facets that have to be aligned to the receiver or heat collection element (HCE). Accurate mirror alignment of faceted solar concentrators maximizes the reflected sunlight intercepting the HCE and can enable the use of a smaller HCE, thereby reducing thermal losses and improving overall collector efficiency. In addition, practical alignment can potentially reduce concentrator installation-fixture accuracy requirements and cost.

Compared with parabolic dish concentrators, practical optical alignment techniques for the accurate alignment of parabolic troughs have not been developed. The relatively short focal lengths and low operating temperature in parabolic trough systems have allowed them to be developed and commercialized with relatively inaccurate alignment by the use of fixtures. Their linear nature has also been a barrier to the development of practical optical techniques. Parabolic dishes, on the other hand, require precise alignment if only to minimize flux hot spots on the solar receiver. In addition, the fact that the facet normals of parabolic dishes conveniently point to the same general location (approximately one focal length behind the dish focus) facilitates alignment.

Accurate alignment of concentrating collectors by the use of fixtures is extremely difficult. Error stackup and indeterminate effects such as thermal expansion make the use of fixtures challenging for precise large optical systems. Although fixtures have been used with parabolic dishes, only optical techniques, which inherently account for error stackup and other factors, have provided the required alignment accuracy. Where optical techniques have been used to measure the alignment of fixture-aligned parabolic troughs, significant misalignment has been reported [5,6]. Mechanical fixtures also do not lend themselves to checking alignment after installation.

To align parabolic dishes, the Jet Propulsion Laboratory (JPL) developed distant observer and distant light source techniques [7,8]; alignment of solar furnace mirrors by the use of a laser was used at the University of Minnesota; [9] and McDonnell Douglas Aircraft Corp. developed and implemented a video-based technique for mirror characterization and facet alignment [10]. Sandia National Laboratories (SNL) further developed variations on the JPL distant light source technique to enable near alignment and daylight alignment by the use of color targets and video cameras [11–14]. With these techniques differences between theoretically calculated and optically measured image positions are used to guide alignment.

Despite the relatively advanced state of commercialization of parabolic troughs, optical alignment is undeveloped. One of the early concepts proposed utilizing reflected images in the mirrors but was never developed [15]. The use of lasers to statistically determine optical accuracy and mirror alignment has received the most attention [5,16], and an approach based on stereoscopic photography has shown promise [6,17]. SNL has used the distant observer technique to align LS-2 trough facets as part of its HCE performance characterization [18]. Unfortunately, trough spacing requirements do not permit the use of the distant observer technique within a trough field. The laser and stereoscopic techniques are also complex, require sophisticated equipment and setup, and are impractical for the staggering number of mirrors in a trough solar power plant.

The ideal mirror alignment technique for any concentrating solar collector would: (1) be simple to set up and implement; (2) use a minimum of sophisticated hardware; (3) not require removal of the receiver/HCE; (4) not require sun or other restrictive weather conditions; (5) not require line-of-sight to a distant observer or light source; and (6) permit accessibility to the mirrors for adjustments [12]. The mirror alignment technique presented here was

Contributed by the Solar Energy Engineering Division of ASME for publication in the JOURNAL OF SOLAR ENERGY ENGINEERING. Manuscript received November 11, 2005; final manuscript received June 5, 2006. Review conducted by Abraham Kribus.

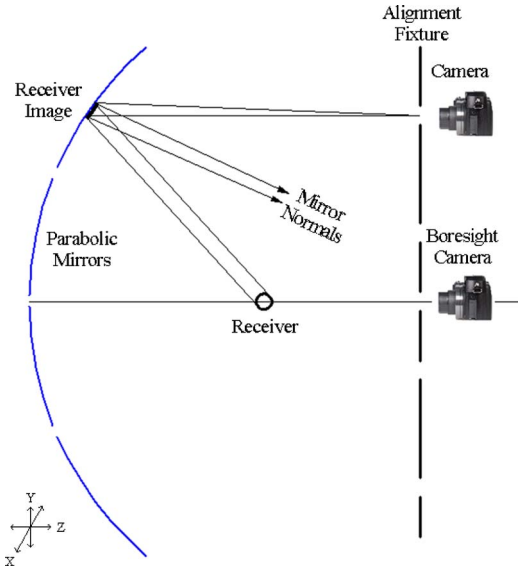

Fig. 1 Schematic illustrating the TOP alignment technique. Accurately positioned cameras on an alignment fixture measure the position of the HCE image in the mirror. The boresight camera is used to align the fixture, HCE, and trough concentrator. The mirror is aligned to superimpose the HCE image onto the theoretically calculated image position.

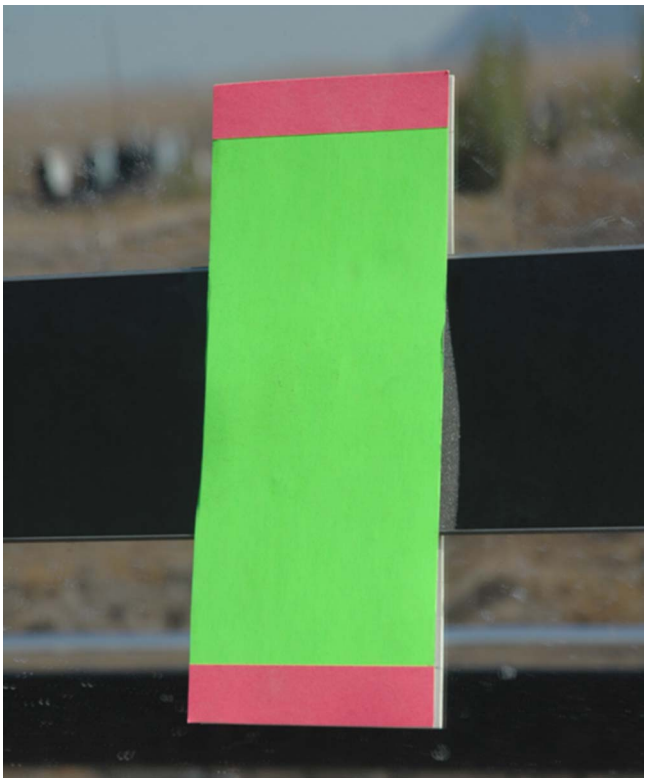

Fig. 2 Photograph of a "boresight gauge" used to boresight the middle camera, HCE, and trough. A foam pad squeezes between the center two mirrors and accurately holds the color sight in position. The green center contrasts with the red edges and is 0.147 m long. The green center was sized to just be hidden from the camera by the HCE when on axis, but can be readily seen when off axis.

derived from practical alignment techniques developed for parabolic dishes for a number of dish systems [11–14]. The color target technique developed in Ref. [13] for the Advanced Dish Development System (ADDS) is similar to the theoretical overlay photographic (TOP) approach presented here [19].

Top Alignment Approach

Figure 1 is a schematic of a trough concentrator and illustrates the basic principles of the theoretical overlay photographic (TOP) alignment approach. An alignment fixture is placed at a convenient distance from the trough collector. For the LS-2 module in our studies, the distance is approximately 10.4 m (34 ft). This distance is close enough to be within the rows in a power plant, but far enough away so that a camera can see an entire module of 20 mirrors without significant fisheye distortion of the image. The trough is pointed horizontally toward the fixture, which is essentially a pole with five cameras accurately positioned along it. The middle camera serves to "boresight" the fixture on the trough. The trough is positioned horizontally (±1 deg) in elevation using its open-loop tracking encoder feedback and the fixture is positioned vertically (±2 deg) with levels. Using boresight gauges mounted between the inner mirrors, Fig. 2, the center camera is bore sighted on the HCE and trough by raising and lowering the fixture. The boresight gauge is designed for simple and accurate installation from the ground and facilitates balancing color top to bottom above and below the HCE to position the alignment fixture on axis with the HCE and mirror array. Images from the other four cameras are then used to align the five mirrors in each of the four rows in the module. Each camera records the location of the HCE image in each mirror in a digital photographic image. The HCE image location in the photograph is then compared to the theoretical projected image location by overlaying the two images. Mirrors are then adjusted to bring the measured image to coincide with the theoretical image. With this approach it is possible to make adjustments and observe real time feedback or to post-process the information and subsequently prescribe adjustments to each mirror mount.

For our proof-of-concept tests we used one camera position per mirror row. It was located to coincide with the center of the row to minimize the effects of mirror facet focal length errors and the impact of mirror mount distortions on the images. We adjusted mirror aim by adding shim washers between the mirror and mounting frame until the images visually coincided. The accuracy of this technique could potentially be enhanced by the use of additional cameras or camera positions, or by the use of computational comparisons of the actual and theoretical images. The difference between the theoretical and measured HCE image edge locations as seen by the camera can be used to measure the vertical component of mirror slope error magnitude and direction for each corresponding image pixel location in the mirror. By taking images at multiple locations per row, this technique could be used to optically characterize individual mirrors or mirrors on modules with high spatial resolution. Figures 3 and 4 show two sets of image overlays (*a*) before and (*b*) after alignment on the LS-2 module at the National Solar Thermal Test Facility (NSTTF) in Albuquerque, NM.

In large-scale commercial applications, we envision a trailer-mounted camera fixture being towed between rows. Surveying technology like that used to plow straight rows for agriculture would establish the correct distance to the trough row being aligned. A field crew would install and remove survey guides and boresight gauges while a driver and optical technician would guide the fixture trailer until the middle camera is centered horizontally on a module. After raising or lowering the fixture to boresight the center camera on axis with the HCE and trough module and checking the verticality of the fixture, images would be taken and stored in a database. The fixture would then be driven to the next module and the process repeated. The images would be processed later and work orders detailing alignment adjustments would be created. Alignment adjustments could be

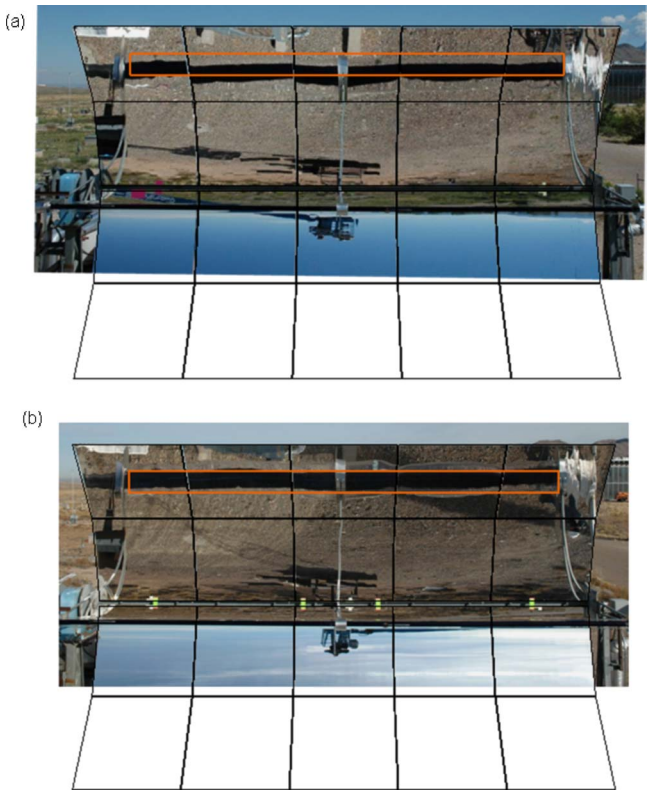

Fig. 3 Theoretical overlay photograph of the LS-2 upper outer row (*a*) before and (*b*) after TOP alignment. Alignment is accomplished by adding shim washers on the side of the mirror in the direction the image needs to be moved.

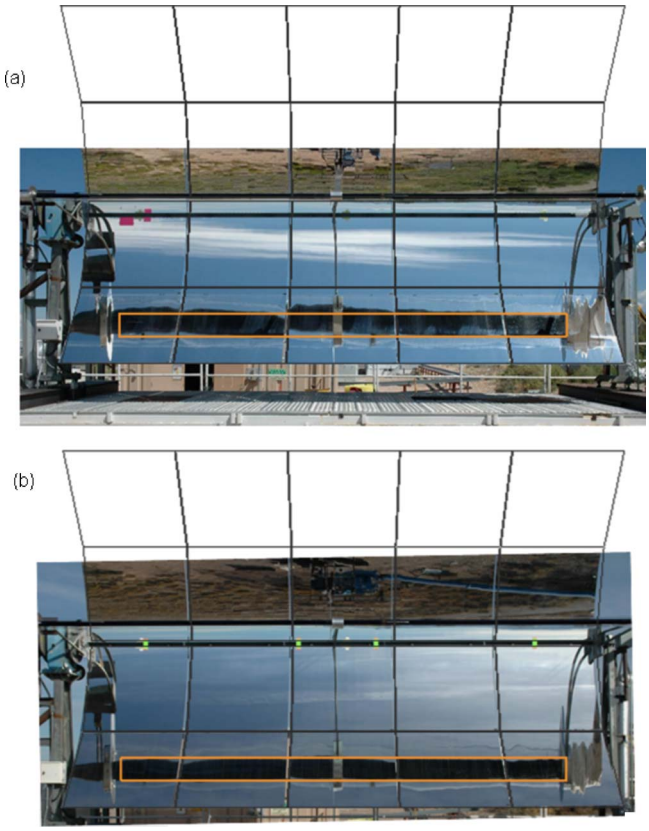

Fig. 4 Theoretical overlay photograph of the LS-2 bottom outer row (*a*) before and (*b*) after TOP alignment. The TOP alignment called for more shims on the left side than the right side of the middle mirror to correct the slanted image.

made when convenient, perhaps even while the plant is operating. As deemed necessary for quality assurance, additional measurements to ensure proper mirror alignment would be made. A possibility for new installations is to stencil theoretical image lines on the mirrors themselves, thereby allowing the installation crew to align the facets during installation from video images.

Theoretical Development

The development of theoretical overlays involves tracing rays from a camera position, to a facet, and then to the edges of the HCE to calculate the theoretical position of the HCE image in the mirrors and then drawing a graphical projection of the image and mirrors as seen by the camera. The equations presented below are based on vector methods used in analytic geometry and are variations on equations used for the alignment of parabolic dishes [11,12].

Consider the coordinate system illustrated in Fig. 5. Alignment errors along the x axis are not considered since the reflected rays still intercept the HCE. Because the trough has no curvature along the x axis, the theoretical image of the HCE is straight along the x axis and the y and z image locations along the mirror are constant. Therefore, to determine the image location as viewed from the camera (A), it is convenient to consider only the z and y vector components. In Fig. 5 the parabola vertex is the origin and the x axis is perpendicular to the plane of the figure. The focal line of the parabola is represented by a point (F). For the LS-2 trough module we defined the vertex as the middle of the module, i.e., the intersection of a vertical line through the middle of the center column of mirrors and the horizontal line along the trough vertex (x axis). The z axis is the optical axis of the trough; a mirror location in space, B, is given by its coordinates (B_x, B_y, B_z); and the HCE is parallel to the x axis and perpendicular to the z axis.

Utilizing the characteristics of the parabola, Fig. 5 shows that for light to be reflected from the sun (S) to the focus (F), the mirror normal for a perfect parabola (vector **BG**) must bisect the angle SBF in the z-y plane, and the distance between points F and G is equal to the distance between points B and F. This relationship is true for all mirror positions (B). Point G is at the intersection of the facet normal and the z axis and is different for each mirror y position.

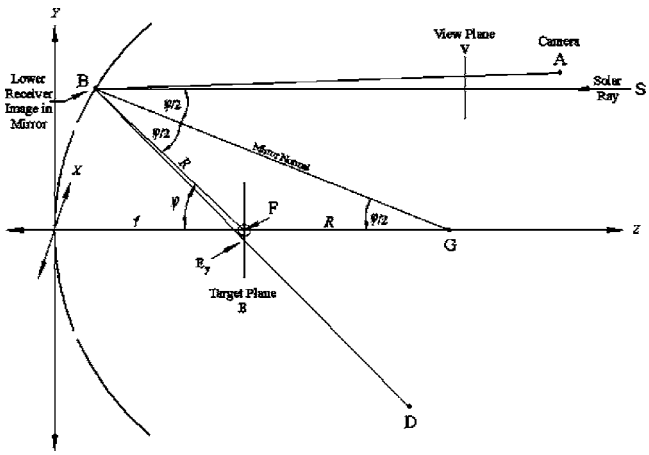

Fig. 5 Schematic showing the coordinate system and locations of the mirror, HCE, target, focus, camera, and the solar rays for calculating the lower receiver edge position in the mirrors.

Useful equations for a parabola applied to the coordinate system in Fig. 5 are

$$B_z = B_y^2/4f \tag{1}$$

and

$$R = 2f/(1+\cos\varphi) \tag{2}$$

where f is the parabola focal length, R is the distance from the parabola to the focus in the z-y plane, and φ is the mirror position angle [20].

To determine the location of the image of the lower receiver edge in the mirror (B) as seen by the camera (A) in Fig. 5, the reflected vector **BD** from the mirror tangent to the bottom edge of the HCE can be iteratively calculated using the vector **BA** from the camera to the mirror and the mirror normal vector **BG** by the use of the following vector mathematics equation.

$$\mathbf{BD} = 2\left(\frac{\mathbf{BA}\cdot\mathbf{BG}}{\mathbf{BG}\cdot\mathbf{BG}}\right)\mathbf{BG} - \mathbf{BA} \tag{3}$$

where the x, y, and z components of vectors **BA** and **BG** are

$$BA_x = A_x - B_x, \quad BA_y = A_y - B_y, \quad BA_z = A_z - B_z \tag{4}$$

and

$$BG_x = G_x - B_x, \quad BG_y = G_y - B_y, \quad BG_z = G_z - B_z \tag{5}$$

respectively. The dot products in Eq. (1) are

$$\mathbf{BA}\cdot\mathbf{BG} = BA_x \times BG_x + BA_y \times BG_y + BA_z \times BG_z \tag{6}$$

and

$$\mathbf{BG}\cdot\mathbf{BG} = BG_x \times BG_x + BG_y \times BG_y + BG_z \times BG_z \tag{7}$$

Equation (3) is based on the law of reflection and has been derived for unit vectors by Biggs and Vittitoe [21]. Note that vector **BD** (from Eq. (3)) has the same magnitude as vector **BA** and that every mirror point along the theoretical parabola (B) has a unique mirror normal that can be determined from the characteristics of a parabola as discussed above.

The location of where vector **BD** intersects the target plane **E** (the plane through the center of the HCE perpendicular to the z axis) corresponding to the bottom edge of the HCE is point E_y and can be calculated by scaling the y component of vector **BD** in accordance with the z component, which is known.

The scale factor between vector **BE** and vector **BD**, **M**, is therefore

$$M = \frac{E_z - B_z}{D_z - B_z} \tag{8}$$

and the y coordinates at the target, point E, is

$$E_y = B_y + M(D_y - B_y) \tag{9}$$

With this set of equations, the location on a mirror (point B) corresponding to where the reflected ray **BD** intersects the edge of the HCE cannot be explicitly solved. It requires an iterative solution to find the mirror position (B) such that vector **BD** is tangent to the HCE. Furthermore because the HCE has a circular cross section, the effective y location corresponding to where vector **BD** is tangent to the HCE depends on the angle in the z-y plane of vector **BD**. For the lower receiver edge image the effective target plane y location (E_y) is

$$E_y = -r/\cos(\varphi + r/R) \tag{10}$$

where r is the HCE tube radius; and R is the distance from the mirror to the focus in the zy plane from Eq. (2).

For the upper receiver image the effective target plane y location (E_y) is

$$E_y = r/\cos(\varphi - r/R) \tag{11}$$

The above equations when iteratively solved determine the y location on the mirror corresponding to the bottom and top edge of the HCE absorber as seen from the camera (A). Because the trough has no curvature along the x axis, the image of the HCE is straight along the x axis. Assuming the HCE length is the same as the module length (effectively the case on the LS-2 since bellow heat shields are located even with the mirror edges), the theoretical x locations in the mirrors corresponding to HCE ends (heat shield locations) can also be iteratively calculated. Solving the above equations for both sides and ends of the HCE gives the theoretical corner positions on the mirrors of the reflected image as seen by the camera of perfectly aligned parabolic mirrors.

The theoretical overlay is the calculated two-dimensional projection of the mirrors and theoretical HCE image (determined above) as seen by a camera at point A. In a camera, the projected image is inverted through lenses onto a detector. For this analysis, the mirror and HCE image coordinates are projected onto a view plane (**V**) between the camera and trough. Because the theoretical image and photograph when overlaid are scaled to match dimensionally, the view plane position (and therefore the size of the theoretical overlay) is not important. In Figs. 1 and 5 the camera is shown pointed parallel to the z axis and perpendicular to the view plane (**V**). In this case the x and y coordinates for the image and facet corners in the view plane (**V**) can be calculated by simply scaling the x and y image and mirror coordinates to the relative z component distances between the camera to view plane vector and camera to facet or image point vectors. If the camera is pointed elsewhere, such as the module vertex, it is convenient to use Cartesian/cylindrical coordinate transformations to align the camera and view plane axis with the transformed z axis to scale the view plane coordinates.

LS-2 Trough Alignment

The LS-2 trough collector is one of three LUZ concentrator designs fielded at the nine solar electric generation systems (SEGS) power plants in southern California. The LS-2 features a central torque tube and truss mirror supports. A module consists of 20 thermally slumped, parabolic-contoured, low-iron, back-silvered glass mirrors and two heat collection elements. The aperture is 5 m rim-to-rim and is nearly 8 m wide [1,2].

Because the LS-2 trough module at the NSTTF is mounted on a rotating platform to facilitate performance measurements, our proof-of-concept alignment fixture was mounted on a stand to compensate for the additional height (Fig. 6). The fixture consists of a heavy-duty tripod on which a 2.5 cm × 7.5 cm (1 × 3 in.) aluminum rectangular tube was mounted. Aluminum Unistrut channel and five angle brackets provide adjustable camera mounts. Inner row camera positions are 0.729 m from the center camera position and the outer camera positions are 1.970 m from the center. These positions correspond to the facet center location for each row, which minimizes the effect of facet focal length variations on alignment. Care was taken to accurately locate the camera focus at the prescribed locations.

For these tests, a Nikon D70 digital camera with an 18–70 mm focal length lens was used. At 10.4 m (34 ft) the camera field of view covered the entire module at a focal length setting of 26 mm. At focal length settings of less than about 22 mm needed to see the entire module at less than about 8 m (26 ft), fisheye distortion of the image was detectable. For most of the tests, the camera was sighted parallel to the z axis by visually framing the module and aiming at the center of the corresponding row. Other tests were performed with the cameras pointed toward the trough vertex with consistent results. As can be seen in Figs. 3 and 4, the theoretical projections accurately match the camera image. Even with the limited-capability image overlay software used in these proof-of-concept tests, we were able to obtain repeatable and precise align-

Fig. 6 Photograph of the alignment fixture and LS-2 concentrator on the rotating platform at the NSTTF. The camera is mounted at the boresight position.

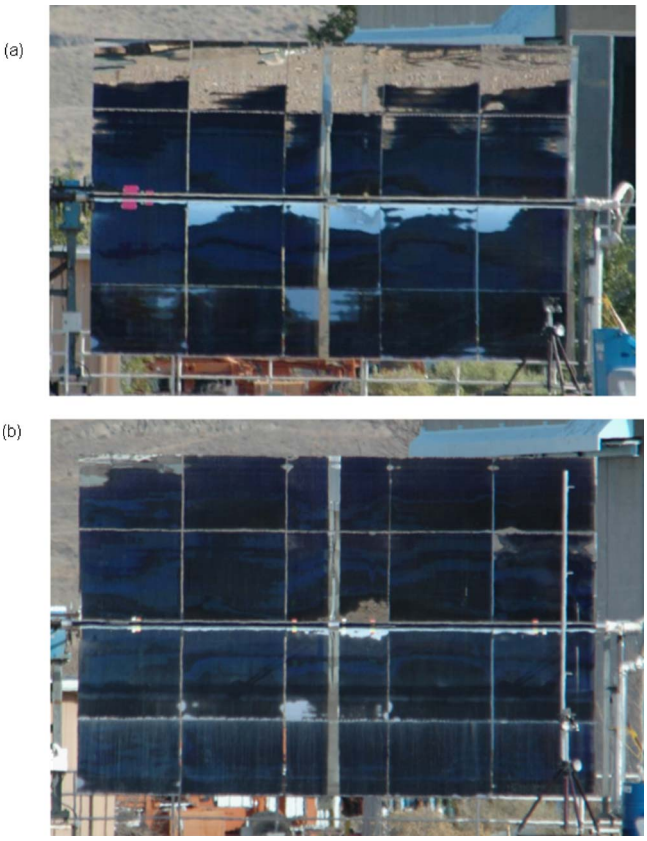

Fig. 7 Distant observer photographs of the LS-2 module at the NSTTF (*a*) prior to and (*b*) after TOP alignment. Because the bottom mirror rows reflect the sky and the top mirror rows reflect the ground, misaligned regions appear blue on the bottom and brown on top. The distance from the camera to the trough vertex is approximately 460 m (1507 ft).

ment. In the proof-of-concept alignment test, all of the mirror alignment shim washers were removed and the module was characterized with both the TOP and distant observer techniques. For the distant observer, rather than aiming the trough by maximizing the amount of black seen in the mirrors, the trough was bore sighted to the HCE using boresight gauges similar to those used to boresight the TOP camera fixture. The TOP approach was then used to determine which mounts needed shim washers. After three iterations the module was aligned. (With experience, we expect the number of iterations can be reduced to one.) Figure 7 shows the (*a*) before and (*b*) after distant observer images of the LS-2 trough and nearly perfect distant observer alignment obtained with the TOP approach. As can be seen by comparing the theoretical overlay photographs in Figs. 3(*a*) and 4(*a*) with the distant observer photograph in Fig. 7(*a*), correlation between the two methods is remarkable. It is important to note that the NSTTF LS-2 as assembled met design specifications. Figure 7(*a*) shows the ability, or lack thereof, of using mechanical fixtures to accurately align mirrors.

The TOP alignment accommodates the four-point mounts utilized on the LS-2. For example, the middle mirror in Fig. 4(*a*) clearly shows a slanted HCE image before alignment which was readily accommodated by adding more spacers to the left side than the right.

Various tests were conducted to determine repeatability and error sensitivity. Testing established that the boresight position is easily repeatable within ±5 mm and that overlay results are repeatable day to day. The effect of the module being rotated around the *y* axis relative to the fixture by rotating the platform 5 deg was also evaluated. Although, this distorts the image relative to the theoretical overlay (the photograph appears large on one side and small on the opposite side), because the theoretical image is still centered in the facets, good estimates of needed adjustments can still be made. For the same reason, results are also insensitive to the distance from the camera to the trough within approximately ±0.5 m (1.6 ft). Testing also showed minimal structural deflections when the LS-2 was rolled over to point in the opposite direction. Image movements from shim washer thicknesses corresponding to approximately 2 mrad of tilt were readily detectable. Our testing showed the TOP alignment has enough resolution to accommodate half-thickness (1 mrad) washers for even more precise alignment, but because they are not used at the SEGS plants and our error analysis (below) determined thinner washers would be of little benefit, they were not used.

Based on these results we are designing and building a "field deployment prototype" alignment fixture. It utilizes five carefully mounted and adjusted fixed video cameras, National Instruments (NI) Vision image processing and analysis software for LabVIEW, and a trailer-mounted self-leveling fixture. For bore sighting an electric actuator raises and lowers the fixture. With the image analysis features in NI Vision, automated bore sighting and the elimination of the boresight gauges may be feasible. Drive by alignment checks in which entire rows of troughs are characterized without stopping may also be possible.

TOP Alignment Error Analysis

There are three primary sources of error that affect alignment accuracy with the TOP approach: (1) mirror location errors; (2) image location errors; and (3) target location errors. Mirror location errors refer to differences between the theoretical mirror location and its actual location. Image location errors refer to errors in centering the photographic image on the theoretical image, and target location errors are errors in positioning the target and camera(s) relative to the concentrator.

Because the HCE receiver serves as the target, and the cameras, HCE, and mirrors are bore sighted together, errors associated with the target location are minimized. In addition, if the HCE is not positioned straight (parallel to the *x* axis in the *y* direction) this

Table 1 Estimated image position uncertainties for LS-2 trough concentrator TOP alignment

Error	Inner row uncert. (±mm)	Outer row uncert. (±mm)
Mirror position, x (±4 mm)	0	0
Mirror position, y (±4 mm)	4	4
Mirror position, z (±4 mm)	0	0
Overlay image position, y (±10 mm)	10	10
Image position, y (±8 mm)	8	8
Bore site position, x (±50 mm)	0	0
Bore site position, y (±5 mm)	5	5
Bore site position, z (±50 mm)	0	0
Camera position, y (±2 mm)	2	2
Trough/fixture perpendicularity (±3 deg)	1	3
Total mirror position uncertainty (mm)	30	32
Total root-sum-square uncertainty (mm)	14.5	14.8

becomes evident during the bore sighting step. In such a case, the technician would note that it needs to be repositioned and move on. Gauging to ensure correct positioning of the HCE in the z direction is another recommended quality assurance step. It is also possible that HCE position could be offset from the trough optical axis. In this event, asymmetric mirror mount adjustments would serve as a flag to check for HCE offset. The HCE borosilicate glass envelope refracts the image of the receiver and causes it to appear slightly smaller. For this study, this effect was not taken into account. Because the bore sighting references the HCE envelop, but aligns to the receiver tube, the concentricity of the receiver within the glass envelope is a potential issue. Modules with badly warped HCEs should not be aligned by this method.

Table 1 is a summary of our estimated uncertainties that can contribute to alignment errors with the TOP alignment technique. These are 95% confidence estimates of what is reasonably achievable in the field extrapolated from our experience with the LS-2 alignment testing presented above. Uncertainties are expressed in terms of displacement (mm) of the HCE image on the mirrors. For example, if the mirror position is off in the x direction (along the length of the trough) there are no alignment uncertainty consequences. However, if it is off in the y dimension by ±4 mm, uncertainties of ±4 mm result in where the HCE image is seen in the inner and outer mirrors. Mirror position errors in the z direction only affect the focal distance and have no impact on alignment since the receiver image is still centered in the mirror. Uncertainties were determined by calculating the difference between the theoretical image position with and without errors.

Sensitivity of the image position to facet misalignment was similarly evaluated by introducing nominal alignment errors and then evaluating the position of the resulting theoretical image. For a nominal misalignment error of 2 mrad, the resulting displacement of the theoretical image is 21 mm/mrad on the outer row mirrors and 18 mm/mrad on the inner row mirrors. The overall additive alignment uncertainty from Table 1 is, therefore, less than 2 mrad for both the inner and outer row mirrors. If the uncertainties in Table 1 are representative of a 95% confidence, then the 2 mrad additive alignment uncertainty estimate is greater than 2 SD and the alignment error standard deviation is better than 1 mrad. Because the root-mean square (rms) slope errors of the LS-2 mirrors are greater than 2 mrad, there is little to be gained by improving on the accuracy of this technique [22].

Structural deflections of the HCE and mirrors between the alignment position and tracking can introduce alignment errors. If the deflections and their effect on alignment can be determined, it is possible to "bias align" the mirrors for any specified orientation by introducing deflection compensation adjustments into the overlays. Special structural deflection tests in which the TOP fixture is supported above the trough can be used to validate structural/optical analysis models, measure gravity induced optical errors, and calculate overlay biases. On the ADDS parabolic dishes gravity induced structural deflections were optically measured with a color $2F$ alignment technique [14].

An assumption in the error analysis is that mirror slope errors are random normal in nature. Because sampling is spatially limited to the center region of the mirrors (mirror locations corresponding to the edges of the HCE receiver image as seen by the camera), if the mirror has systematic slope errors alignment can be skewed. The most general systematic error is focal length errors. Sampling the center region of the mirror minimizes alignment errors caused by facet focal length variations. It is interesting to note that the width of the HCE image in the mirrors provides a measure of facet focal length. The size of the reflected image was used to focus stretched-membrane facets on the Cummins Power Generation CPG-460 dish concentrator, and to measure focal length of the ADDS mirrors [12,13]. Other systematic errors are also possible. Laser ray-tracing techniques or a scanning TOP should be used to characterize a statistically significant sample to make sure systematic bias errors do not bias alignment accuracy. Although published ray-trace data show that systematic errors exist on LS-2 type mirrors, they indicate that sampling the center of the mirror is a good location [5]. The results presented here also suggest that systematic slope errors are not an issue, but additional studies are planned. If needed, the use of bias alignment approaches or additional camera positions are potential approaches for addressing systematic slope errors.

It should be pointed out that the TOP technique aligns all of the mirrors in a module to the HCE. It does not guarantee all of the modules on a drive are aligned with each other. Some of the bore sighting techniques used in the TOP approach could be adapted to guide module alignment. In addition, some of the mirror mounts on the LS-2 use moment joints, and if not perfectly aligned with the mounting flange can optically distort the mirror. When aligning dish mirrors with the benefit of direct optical feedback of distant light source images, mirror distortion could readily be observed on more compliant mounts attached to stiffer facets than used on the LS-2. Misaligned areas on the LS-2 module seen in the distant observer image in Fig. 7(*b*) are caused by mirror mounts. Careful mirror mount design to avoid mirror distortion is another area for improvement.

Conclusions

An innovative alignment technique based on overlaying theoretical images of a trough module onto carefully surveyed photographs has been invented and investigated. The TOP technique, as with dish optical alignment approaches, uses differences between theoretically calculated and optically measured image positions to guide mirror alignment. The TOP technique satisfies all of the requirements of an ideal alignment process. It uses relatively low technology equipment, inherently aligns the mirrors to the HCE, and can be implemented day or night within the rows of commercial trough power plants. It is also adaptable for use in new installations, mirror replacement, and for characterizing gravity-induced optical errors. Alignment accuracy should be better than the optical accuracy of the mirrors themselves, therefore enabling the best possible optical performance.

The TOP alignment technique was validated on the rotating platform at the NSTTF. To further the approach for commercial applications, a trailer-mounted fixture with five fixed cameras, image overlay analysis software, and overall process streamlining is being developed. The techniques employed here can also potentially be extended to align trough modules to each other within drive strings or employed to fully characterize the optical accuracy of trough mirrors and modules.

Accurate alignment of faceted solar concentrators is important for achieving full performance potential and is a critical requirement for parabolic dishes. Even for parabolic troughs, accurate mirror alignment helps reduce spillage losses in existing facilities,

and can improve the concentration ratio and potentially reduce installation costs in new designs. Other lessons learned in dish technology development are relevant to troughs and visa versa.

Acknowledgment

SAND2005-7017J. This work is supported by the U.S. Department of Energy under Contract No. DE-AC04-94-AL85000. The authors would like to acknowledge the contributions of Daniel Ray and J.J. Kelton who fabricated the alignment fixture.

Nomenclature

A = camera point, (x,y,z) (m)
B = mirror position, (x,y,z) (m)
D = point in space of reflection of camera to mirror ray (x,y,z) (m)
F = focal line and HCE centerline (x,y,z) (m)
G = point along optical axis (x,y,z)
M = scale factor between vectors **BE** and **BD**
S = sun position (x,y,z) (m)
f = parabola focal length (m)
r = HCE tube radius (m)
R = distance from parabola to focus in the zy plane (m)
E = target plane position (x,y,z) (m)
V = view plane position (x,y,z) (m)
BA = camera to mirror vector (x,y,z) (m)
BD = mirror reflection vector (x,y,z) (m)
BG = mirror normal vector (x,y,z) (m)
φ = mirror position angle (rad)

Subscripts

x,y,z = Cartesian coordinates (m)

References

[1] Price, H., Lupfert, E., Kearney, D., Zarza, E., Cohen, G., Gee, R., and Mahoney, R., 2002, "Advances in Parabolic Trough Solar Power Technology," ASME J. Sol. Energy Eng., **105**, pp. 288–293.
[2] Dudley, V. E., Kolb, G. J., Sloan, M., and Kearney, D., 1994, "Test Results SEGS LS-2 Solar Collector," SAND94–1884, Sandia National Laboratories, Albuquerque, NM.
[3] Geyer, M., ed., 2005, "Solar Power and Chemical Energy Systems Solar PACES," Annual Report 2004, Deutsches Zentrum fur Luft-und Raumfahrt, Köln, Germany.
[4] Kistner, R., Grethe, K., Geyer, M., and Nebrera, J. A., 2004, "The Progress of the AndaSol Projects in Spain," *Proceedings of the 12th Solar PACES International Symposium*, Oaxaca, Mexico, October 6–8.
[5] Wendelin, T., 2004, "Parabolic Trough Optical Characterization at the National Renewable Energy Laboratory," *Proceedings of the DOE Solar Program Review Meeting*, Golden, CO, October 25–28, Paper No. DOE/GO-102005–2067.
[6] Lupfurt, E., Pottler, K., Ulmer, S., Riffelmann, K. J., and Schiricke, B., 2005, "Parabolic Trough Analysis and Enhancement Techniques," *Proceedings of ISES2005 2005 International Solar Energy Conference*, Orlando, FL, August 6–12.
[7] Livingston, F. R., 1985, "Activity and Accomplishments in Dish/Stirling Electric Power System Development," DOE/JPL-1060–82, Pasadena, CA.
[8] Selcuk, M. K., 1995, "Parabolic Dish Test Site: History and Operating Experience," DOE/JPL-1060-84, Pasadena, CA.
[9] Diver, R. B., Carlson, D. E. E., Macdonald, F. J., and Fletcher, E. A., 1983, "A New High-Temperature Solar Research Furnace," ASME J. Sol. Energy Eng., **105**, pp. 288–293.
[10] Blackmon, J. B., and Stone, K. W., 1993, "Application of the Digital Image Radiometer to Optical Measurement and Alignment of Space and Terrestrial Solar Power Systems," *Proceedings of the 28th IECEC*, Atlanta, GA, August 8–13, Paper No. 93217.
[11] Diver, R. B., 1992, "Mirror Alignment Techniques for Point-Focus Solar Concentrators," SAND92–0668, Sandia National Laboratories, Albuquerque, NM.
[12] Diver, R. B., 1995, "Mirror Alignment and Focus of Point-Focus Solar Concentrators," *Solar Engineering 1995: Proceedings of the ASME/JSME/JSES International Solar Energy Conference*, Maui, HI, March.
[13] Andraka, C. E., Diver, R. B., and Rawlinson, K. S., 2003, "Improved Alignment Technique for Dish Concentrators," *International Solar Energy Conference Proceedings*, Kohala Coast, HI, March 15–18.
[14] Steffen, B. J., Andraka C. E., and Diver R. B., 2003, "Development and Characterization of a Color 2F Alignment Method for the Advanced Dish Development System," *International Solar Energy Conference Proceedings*, Kohala Coast, HI, March 15–18.
[15] Wood, R. L., 1981, "Distant Observer Techniques for Verification of Solar Concentrator Optical Geometry," UCRL53220, Lawrence Livermore National Laboratory, Livermore, CA.
[16] Butler, B. L., and Pettit, R. B., 1977, "Optical Evaluation Techniques for Reflecting Solar Concentrators," Proc. SPIE **144**, pp. 43–49.
[17] Shortis, M. R., and Johnston, G., 1997, "Photogrammetry: An Available Surface Characterization Tool for Solar Concentrators, Part II: Assessment of Surfaces," ASME J. Sol. Energy Eng., **119**, pp. 281–291.
[18] Moss, T. A., and Brosseau, D. A., 2005, "Test Result of a Schott HCE Using a LS-2 Collector," *Proceedings of ISES2005 2005 International Solar Energy Conference*, Orlando, FL, August 6–12.
[19] Diver, R. B., Andraka, C. E., Rawlinson, K. S., Moss, T. A., Goldberg, V., and Thomas, G., 2003, "Status of the Advanced Dish Development System Project," *International Solar Energy Conference Proceedings*, Kohala Coast, HI, March 15–18.
[20] Duffie, J. A., and Beckman, W. A., 1974, *Solar Energy Thermal Processes*, Wiley, New York, Chap. 8.
[21] Biggs, F., and Vittitoe, C. N., 1976, "The Helios Model for the Optical Behavior of Reflecting Solar Concentrators," SAND76–0347, Sandia National Laboratories, Albuquerque, NM.
[22] Wendelin, T., and Gee, R., 2004, "Optical Evaluation of Composite-Based Reflector Facets for Parabolic Trough Concentrators," *Proceedings of Solar 2004 Conference*, ISES 04, Portland OR, July 11–14.